The Role of Ice Shelf Ocean Interaction in the ECCO2 Data Synthesis

Michael Schodlok

Jet Propulsion Laboratory, California Institute of Technology, Pasadena

OS31C-1298

ECCO2 Data Synthesis:

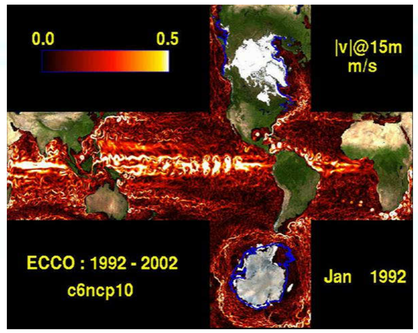

The Estimating the Circulation and Climate of the Ocean, Phase II (ECCO2) project aims to synthesize available global-ocean and sea-ice data with a state-of-the-art ocean general circulation model at eddy-permitting resolution. An ECCO2 data synthesis is obtained by least-squares fit of a global full-depth ocean and sea-ice configuration of the Massachusetts Institute of Technology general circulation model to the available satellite and in-situ data using the Green's functions method.

Model configuration for optimised solution (CS):

- Cube sphere projection: 6 faces x 510 x 510 grid cells
- Mean horizontal resolution ~ 18 km
- 50 vertical levels with thicknesses from 10 m to 456 m
- Volume-conserving
- Bathymetry: Blend GEBCO + Smith/Sandwell 2004
- Forcing: NCEP/ECMWF/ERA40/CORE/ECCO-GODAE winds
- Initial conditions: WOA05
- Period of model run used: Jan 1992 – Dec 2006

Model improvements through implementation of Ice Shelf Ocean Interaction

Model configuration for Ice Shelf Ocean Interaction:

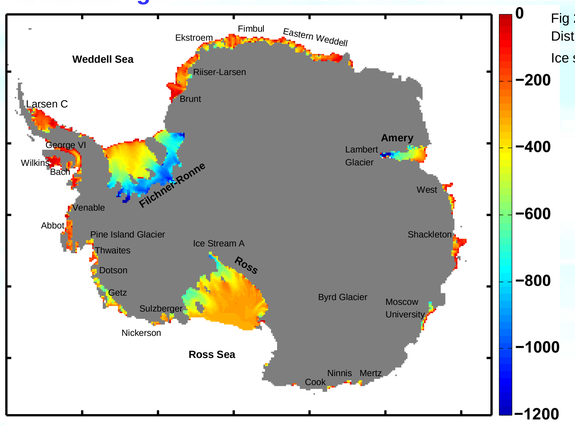

Fig 2.: Distribution of Ice shelf Thickness

- Cube Sphere projection: 496 x496 x 50 grid cells
- Bathymetry: Smith and Sandwell 2008
- Ice Shelf Thickness: ICESat/GLAS
- Water Column Thickness: BEDMAP
- Forcing: as optimised solution (CS)
- Boundary Conditions: monthly means from the global optimised solution
- MITgcm ice shelf package: Losch (2008)
- Integration Period: Jan 1992 – Dec 2006

Model differences (with and without ice shelves):

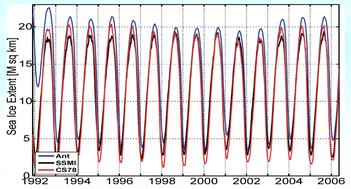

Fig. 3: Time Series of Antarctic sea ice extent for the integration period 1992 to 2007 for runs with ice shelf ocean interaction (Ant), without ice shelf ocean interaction (CS78 – optimised global ECCO2 solution) compared to SSM/I data

Changes at first glance:

- Summer sea ice extent (with ice shelves) improved towards observed values
- Winter sea ice extent (with ice shelves) is higher than observed due to an increase in sea ice production and export
- Sea ice thicknesses increased due to freshwater input from sub ice shelf cavities.
- difference in summer (Fig 4. left) due to underestimation of sea ice in case without ice shelves
- larger increase and wider spatially distributed compared to Hellmer (2004)
- Drake Passage transport increased by about 5 Sv

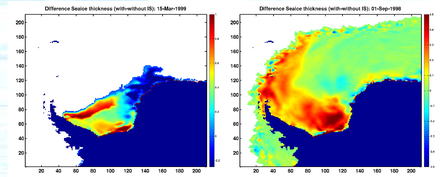

Fig. 4: Snapshot of sea ice thickness differences in summer (left) and in winter (right) in the Weddell Sea between model run with and without ice shelf ocean interaction. Note the difference of the scale; differences in summer are larger than in winter.

Circumpolar Freshwater Fluxes (FWF):

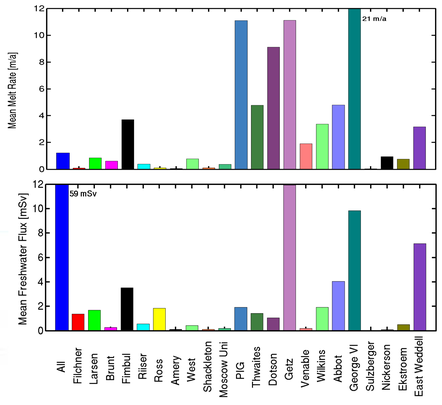

Table 1: Ice Shelf Area, Freshwater Flux, and Melt Rate. PIG: Pine Island Glacier, EWIS: Eastern Weddell Ice Shelves (incl. Lazarev IS), Moscow U: combination of Moscow University and Totten IS.

	Size M SqKm	FWF [mSv]	Melt Rate[m/a]
All	15.09	59.79 ± 7.44	1.23 ± 0.15
Filchner	4.38	1.37 ± 0.73	0.09 ± 0.05
Larsen	0.61	1.69 ± 0.39	0.87 ± 0.20
Brunt	0.26	0.26 ± 0.37	0.61 ± 0.82
Fimbul	0.30	3.52 ± 0.91	3.71 ± 0.96
Riiser	0.45	0.55 ± 0.28	0.39 ± 0.20
Ross	4.94	1.84 ± 1.32	0.12 ± 0.08
Amery	0.65	0.11 ± 0.43	0.06 ± 0.21
West	0.17	0.43 ± 0.47	0.79 ± 0.86
Shackletn	0.30	0.10 ± 0.48	0.11 ± 0.49
Moscow U	0.15	0.18 ± 0.28	0.39 ± 0.58
PIG	0.05	1.93 ± 0.76	11.09 ± 4.36
Thwaites	0.09	1.44 ± 0.48	4.80 ± 1.60
Dotson	0.04	1.06 ± 0.19	9.13 ± 1.72
Getz	0.34	11.94 ± 1.45	11.12 ± 1.35
Venable	0.03	0.20 ± 0.14	1.90 ± 1.33
Wilkins	0.18	1.92 ± 0.53	3.37 ± 0.93
Abbot	0.26	4.05 ± 0.62	4.81 ± 0.73
George VI	0.29	9.84 ± 0.73	20.90 ± 1.57
Sulzbergr	0.10	0.01 ± 0.02	0.04 ± 0.08
Nickerson	0.03	0.09 ± 0.05	0.96 ± 0.53
Ekstrøm	0.21	0.52 ± 0.27	0.77 ± 0.41
EWIS	0.71	7.13 ± 1.99	3.17 ±0.88

Fig. 9: Mean melt rates (dh/dt) and freshwater fluxes (FWF) from individual ice shelves (see also Table1). Bottom two figures is an excerpt of the top figures. Freshwater flux is 30 mSv higher than e.g. Hellmer (2004) due to (a) more ice shelves considered in this integration, (b) overestimated dh/dt in the WAIS region, in particularly George VI Ice Shelf due to uncertainties in orography and bathymetry. (Positive values for melting in this case for graphic purposes only)

Model Results: Melt Rates in ECCO2

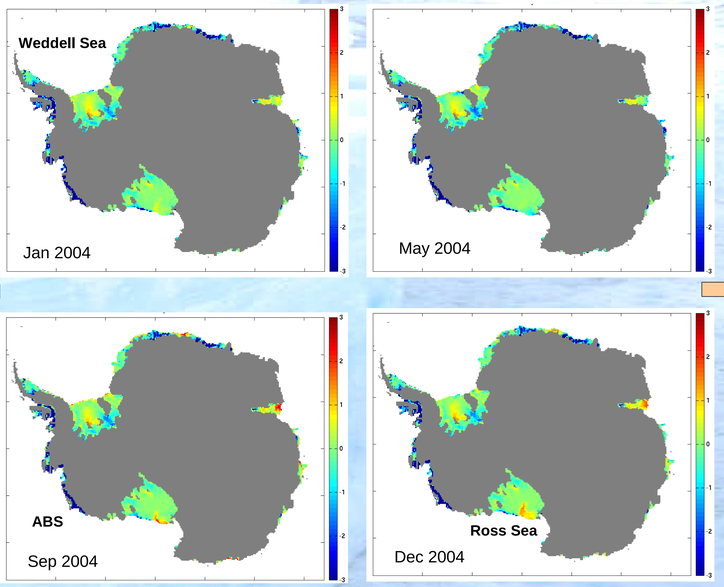

Fig. 5: Horizontal distribution of melt rates dh/dt. Negative values represent melting at the base of the ice shelf and positive values refreezing. Melt rates in the Amundsen Bellingshausen Sea (ABS) exceed the scale of the colour bar (see Table 1 for results). The pattern of melting and freezing is in good agreement with regional studies, e.g. BRIOS: Beckmann et al, 1999, Schodlok (2002).

Weddell Sea:

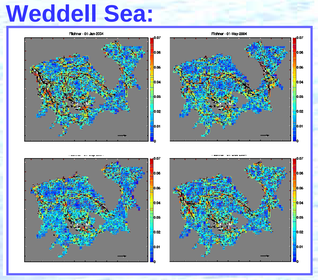

Ross Sea:

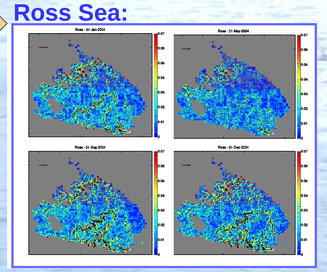

Fig. 6: Mean horizontal velocity distribution in the Filchner Ronne (top) and Ross (bottom) ice shelf cavity. The colours indicate speed, arrows the direction of flow (reference vector 0.1 m/s).

- **pronounced seasonal cycle in melting and freezing pattern**
- **pronounced seasonal cycle in sub ice shelf cavity circulation**
- **Weddell Sea:**
  strong exchange between Filchner and Ronne cavities in winter, less pronounced in summer
  strong inflow into Ronne cavity in summer, less pronounced in winter
- **Ross Sea:**
  pronounced cavity in- and outflow in the western basin in winter and spring
  correlation with melting and freezing pattern (Fig. 5) and thus water mass exchange
  weak exchange of water masses with cavity exterior in autumn/ beginning of winter
- **interannual variability in melt pattern → longer time series necessary**
- **trend in melt rate (reduction) uncertain due to possible misrepresentation of western Antarctic Ice Shelves**

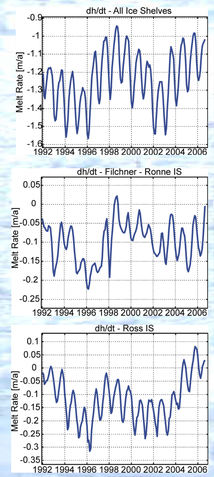

Fig. 7: Melt rate time series for the integration period 1992 to 2006 for all ice shelves (top), Filchner Ronne Ice Shelf (mid), and Ross Ice Shelf (bottom). Note the difference in scale. Negative values depict melting, positive freezing. Pronounced seasonal cycle for all ice shelves with maximum melting in winter and minimum in summer. Melt Rate time series dominated by WAIS ice shelves.

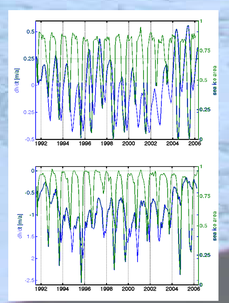

Fig. 8: Mean sea ice area (green) vs mean ice shelf melt rate (blue) in the western part (top) and the eastern part (bottom) of the Ross Sea. In the western part the maxima of melting are lagging the minima of sea ice cover by 2 months. This relationship is less prominent in the eastern part of the Ross Sea. The maximum of freezing in the western part is related to the onset of summer and reduction of sea ice cover. There is no freezing in the eastern part of the Ross Sea. Both can be associated with the in and outflow of water masses into the cavity (see Fig. 6)

Larsen C melt rates: Connection to Larsen B break up in 2002?

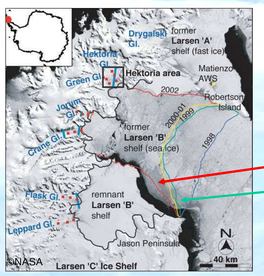

Fig. 11: Satellite Image of Larsen B. Ice Front retreat from 1998 to 2002 is shown as coloured lines.

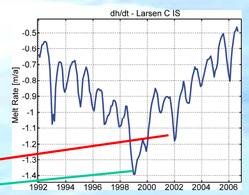

Fig. 10: Time series of melt rate (dh/dt) of Larsen C area. Increase of basal melt rates from the beginning of the time series leads to thinning of ice shelves, thus possibly are pre-conditioning for break up.

- Assumption that melt behaviour is valid for northern Weddell Sea, incl. Larsen B area.
- Melt rate of Larsen C is close to estimates from E. Rignot (0.86 m/a, pers. Comm., 2008)
- Longer time series of melt rates and thorough model evaluation necessary.
- This time series does not explain the break up of Larsen B

Conclusion – ongoing work:

- modeled freshwater fluxes (59 mSv) are higher compared to previous estimates
- possible overestimation of FWF at Amundsen Bellingshausen Sea ice shelves

→ revision of bathymetry and ice shelf thickness in the Amundsen Bellingshausen Sea (P. Holland, pers. Comm., 2008)

→ implementation of ice shelf configuration in the global model domain of ECCO2 for better representation of high latitude processes

References:

Beckmann, A., H.H. Hellmer, and R. Timmermann. A numerical model of the Weddell Sea: large scale circulation and water mass distribution. J. Geophys. Res., 104, 23375-23391, 1999.

Hellmer, H.H., Impact of Antarctic ice shelf basal melting on sea ice and deep ocean properties. Geophys. Res. Lett., 31(10), 2004.

Losch, M., Modeling ice shelf cavities in a z coordinate ocean general circulation model. J. Geophys. Res., 113, C08043, doi:10.1029/2007JC004368, 2008.

MITgcm-Group, MITgcm Release 1 Manual, Online documentation, MIT/EAPS, Cambridge, USA, 2002

Schodlok, M.P., On the spreading of deep water in the Weddell and Scotia Seas, Berichte zur Polar- und Meeresforschung, 432, pp144, 2002

Smith, W.H.F. and D.T. Sandwell, Global sea floor topography from satellite altimetry and ship depth soundings., Science, 277, 1956-1962, 1997.

Acknowledgements: ECCO2 is a contribution to the NASA Modeling, Analysis, and Prediction (MAP) program. We gratefully acknowledge computational resources and support from the NASA Advanced Supercomputing (NAS) Division and from the JPL Supercomputing and Visualization Facility (SVF). Thanks to M. Dinniman, F. Nitsche, and B. Galton-Fenzi for ice shelf thickness and/or bathymetry data.

email: Michael.P.Schodlok@jpl.nasa.gov